J. Cosmet. Sci., 54, 301–316 (May/June 2003)

Analyzing the laser-light reflection from human hair fibers. I. Light components underlying the goniophotometric curves and fiber cuticle angles

F.-J. WORTMANN, *DWI, Deutsches Wollforschungsinstitut e. V., Veltmanplatz 8, 52062 Aachen, Germany,* E. SCHULZE ZUR WIESCHE, *Henkel KGaA, Henkelstrasse 67, 40191 Düsseldorf, Germany, and* A. BIERBAUM, *Fiantec GmbH, Technologiezentrum, Europaplatz, 52068 Aachen, Germany.*

Accepted for publication August 1, 2002.

Synopsis

The consumer may repeatedly over the day apply intensive grooming procedures to maintain and improve hair appearance. Among these, brushing and combing are responsible for changes if not damage to the hair fiber surface. Beneficial or unfavorable changes to the hair surface may furthermore result from any cosmetic treatment. The analysis of laser-light reflection and scattering of human hair fibers is a direct, quick, and non-destructive method to monitor such surface changes. The application of a laser-based, multichannel goniophotometer is described, by which this analysis is based on the determination of the complete angular distribution of reflected light within a sub-second time interval. Systematic investigations of hairs differing in ethnic origin and color show that the goniophotometric curves can be analyzed by assuming three fractions of reflected light, namely, specularly, diffusely, and internally reflected light. Prominent effects are related to changes of the relative intensities of the different light fractions with hair color. The angular intensity distribution for each of the light fractions is well described by a Gaussian distribution. The angular positions of the peaks and their widths are analyzed. From the systematic shift of the intensity peak for specularly reflected light from its expectation angle, the tilt angle of the cuticle cells on the hair fiber surface is determined. All results are discussed with respect to changes along the hair length and for color differences.

INTRODUCTION

The consumer may repeatedly over the day apply intensive grooming procedures to maintain and improve hair appearance. Among these, brushing and combing are responsible for changes if not damage to the hair fiber surface. Changes to the hair surface will furthermore result from any procedure carried out on the hair, be it bleaching, weathering, abrasion, permanent-waving, to give just a few examples. The analysis of

Address all correspondence to F.-J Wortmann.

light reflection and scattering is potentially a direct, quick, and non-destructive method to monitor such changes to the hair surface.

Fundamental investigations of light reflection from hair applied goniophotometry to single or arrays of parallel fibers (1–6). For single fibers this method gives detailed insight into the interaction between light and the fiber surface, and a variety of parameters can be defined in terms of the properties of specularly and diffusely reflected light. However, inherent large variations between individual hairs, be they of color, size, etc., on the one hand, and the long recording time for standard goniophotometric techniques (approx. 15 min), on the other, prevented a broader application (2,6).

For our investigations this limitation of goniophotometry was overcome by adapting a multichannel instrument, developed by Haertl *et al.* (7), with fast access to the complete angular distribution of reflected light from which the intensity distributions for three different components of reflected light can be determined. For a first, fundamental investigation of the methodology, the angular positions and widths of the various components of reflected light and the cuticle angles derived thereof were determined along the length of hairs differing in color and ethnic origin, in order to better understand the connection between hair surface and bulk morphology and light scattering.

DETERMINING LIGHT REFLECTANCE FROM HUMAN HAIR FIBERS

The measurement of light reflectance and scattering from single human hairs, described in this paper, is based on the determination of the angle-dependent intensity of the light from a green laser (λ = 532 nm) reflected from a single fiber. The wavelength was chosen such as to be in that range were the daylight sensitivity of the human eye is at a maximum (8). Figure 1 shows the experimental setup for the investigations.

At the center of the setup, a hair (length: 10 cm) is held horizontally in a special holder at a constant tension of 200 mg and under ambient, though stable, room conditions (approx. 22°C, 50% RH). The holder contains up to ten hairs in parallel and allows vertical movements to select a hair and horizontal movements in order to select the position to be studied.

Three types of hair were investigated, namely brown and blonde Caucasian, and black Asian hair. Each sample was taken from the head of a female volunteer and exceeded in all cases 20 cm in length. The hairs were shampooed (LES 15%, pH 5.5), rinsed, dried, and stored under ambient conditions until usage.

The laser beam (approx. 50 µW) is vertically polarized (see Figure 1) and meets the hair fiber, arranged horizontally, at an incident angle of 40° (beam spot size 100 µm). The detection of the reflected light is conducted in the horizontal plane containing the fiber and the incident light beam with an *O*ptical *M*ulti-Channel *A*nalyzer (OMA), described in reference (7).

The detector contains 167 windows arranged such that each window covers 1°, with an overall range for the recording angle of 6.5° to 173.5° around the center of light scattering and with respect to the direction of the laser beam. The windows are connected to light guides that transform the signals into a rectangular array, where the light intensity distribution is observed by a CCD camera, digitized, and analyzed. The data are corrected for the transmission characteristics of the individual light guides and for

goniophotometry (2), by allowing a large number of measurements in a short period of time. This enables one to arrive at significant results despite the inherent large variability of the hair material.

Due to the nature of the parameters to be discussed here, no calibration of the instrument with respect to luminance (9) was conducted. Influences on the GP curves by diffraction effects are expected at large incidence angles only ($>\approx 60°$) (3).

The surface of hair is not smooth but features cuticle cells in a tile-like arrangement, where the cell scale edges point towards the fiber tip. In the case of human hair, multiple layers of cuticle cells are observed. They amount to about ten layers in the root region and are progressively worn off towards the tip through combing and brushing (10). Figure 3 shows an SEM micrograph of a Caucasian hair of typical appearance. The section originates from the middle part of a medium-length (25 cm), brown hair from a Caucasian female. The hair shows typical, though minor, damage of the scale edges and a few lifted scales due to grooming.

In view of the surface and overall morphological structure of human hair, the reflection of light will be subject to a special type of geometry, which, in turn and with the principles of geometrical optics, leads one to expect three principal components of light reflection, as schematically shown in Figure 4. Such a three component model has been proposed and investigated by Stamm *et al.* (11) and subsequently by Guiolet *et al.* (4).

The model is based on the simplifying, but reasonable assumption that the relevant reflection and refraction processes occur at the air/hair interface. Differences in the refractive indices of the morphological components are considered in a first approximation as being of minor importance.

The incident beam hits the fiber surface in the root-to-tip (RT) direction at the incident angle ϵ_I, which is given with respect to the direction normal to the fiber axis.

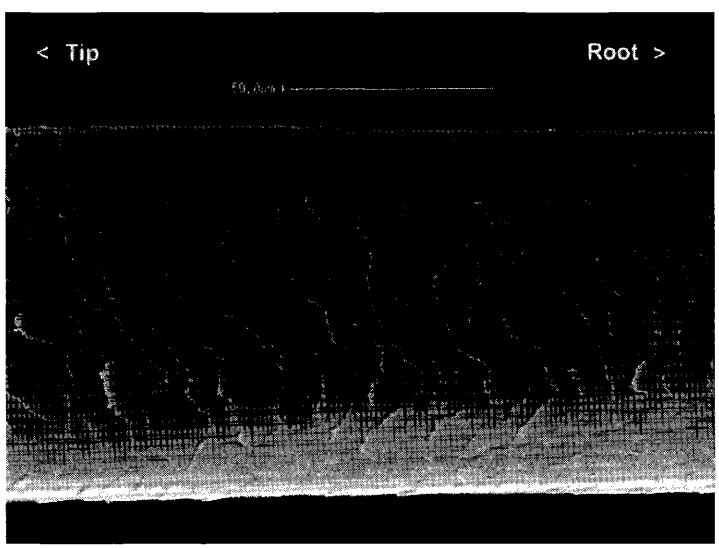

Figure 3. Scanning electron micrograph of a typical Caucasian human hair. The section originates from the middle part of a medium-length (25 cm) brown hair taken from a Caucasian female.

goniophotometry (2), by allowing a large number of measurements in a short period of time. This enables one to arrive at significant results despite the inherent large variability of the hair material.

Due to the nature of the parameters to be discussed here, no calibration of the instrument with respect to luminance (9) was conducted. Influences on the GP curves by diffraction effects are expected at large incidence angles only (>≈60°) (3).

The surface of hair is not smooth but features cuticle cells in a tile-like arrangement, where the cell scale edges point towards the fiber tip. In the case of human hair, multiple layers of cuticle cells are observed. They amount to about ten layers in the root region and are progressively worn off towards the tip through combing and brushing (10). Figure 3 shows an SEM micrograph of a Caucasian hair of typical appearance. The section originates from the middle part of a medium-length (25 cm), brown hair from a Caucasian female. The hair shows typical, though minor, damage of the scale edges and a few lifted scales due to grooming.

In view of the surface and overall morphological structure of human hair, the reflection of light will be subject to a special type of geometry, which, in turn and with the principles of geometrical optics, leads one to expect three principal components of light reflection, as schematically shown in Figure 4. Such a three component model has been proposed and investigated by Stamm *et al.* (11) and subsequently by Guiolet *et al.* (4).

The model is based on the simplifying, but reasonable assumption that the relevant reflection and refraction processes occur at the air/hair interface. Differences in the refractive indices of the morphological components are considered in a first approximation as being of minor importance.

The incident beam hits the fiber surface in the root-to-tip (RT) direction at the incident angle ϵ_I, which is given with respect to the direction normal to the fiber axis.

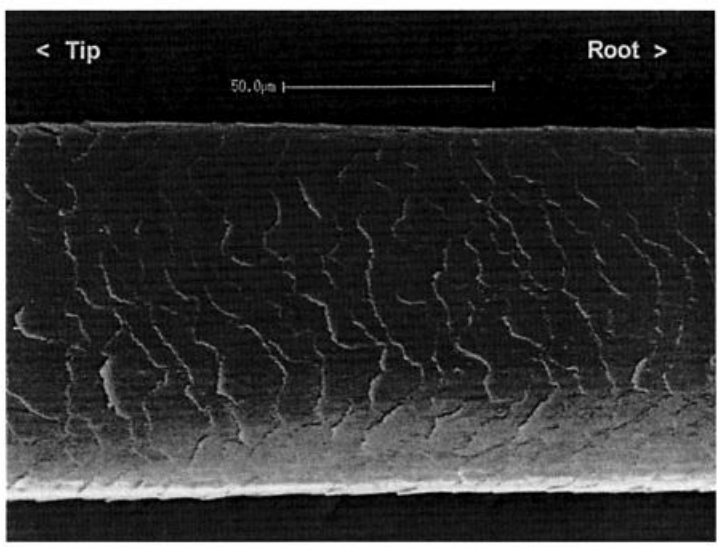

Figure 3. Scanning electron micrograph of a typical Caucasian human hair. The section originates from the middle part of a medium-length (25 cm) brown hair taken from a Caucasian female.

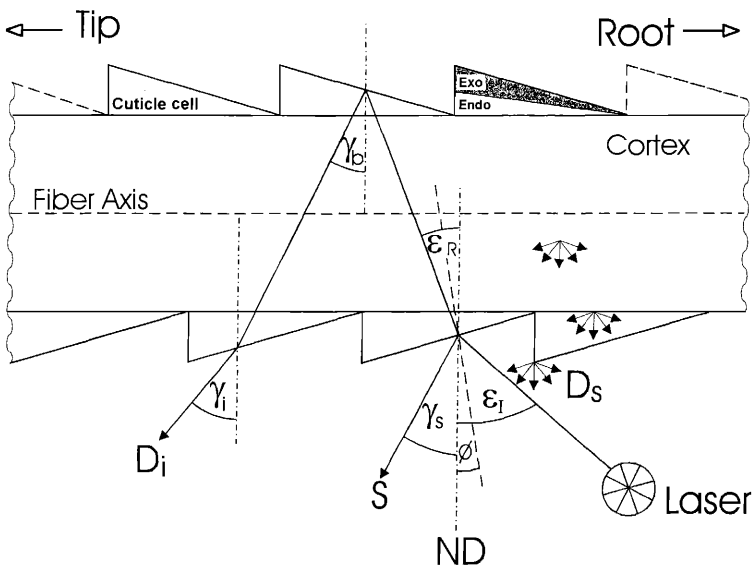

Figure 4. Principles of light reflection and backward scattering on and in a hair fiber, graphically defining the parameters used in equations 1–6. The relevant components of keratin morphology are indicated. Angles were chosen to illustrate the principles of light reflection and refraction, not for physical correctness. ND is the *n*ormal *d*irection with respect to the fiber axis and in the horizontal plane.

A first fraction of light S is *s*pecularly reflected at the receptor angle γ_s:

$$\gamma_s = \epsilon_I - 2\phi \tag{1}$$

where ϕ is the tilt angle of the cuticle cell with respect to the fiber axis. Values for the tilt angle given in the literature are between 2.5° (11) and 3° (1,4,11). For our experimental setup, using an incident angle of $\epsilon_I = 40°$ and assuming $\phi = 2.5°$ leads to an expectation value for the receptor angle of the specularly reflected light of $\gamma_s = 35°$. Analogous geometric considerations apply for light traveling in the tip-to-root (TR) direction (11).

A second fraction of light D_s is *d*iffusely *s*cattered and reflected at and near the fiber surface, namely at surface roughnesses (12), at the various interfaces between the cuticle cell layers of human hair (11), the interface of cuticle and cortex, and at optical imperfections of the cortex, such as voids and inclusions. When the hair is colored, the intensity of light reflected from within the hair is diminished, leading to a decrease in intensity of diffusely reflected light with the darkness of the hair.

If the hair surface would be an ideal, diffuse reflector, scattering would occur omnidirectionally, so that the intensity of the diffusely reflected light would be uniform. Since, in view of Figure 2 and the other GP curves presented below, this is obviously not the case, it can be assumed (11) that the geometrical dimensions of the scattering centers are comparable to or greater than the wavelength of the incident light. Surface structures of suitable dimensions are the cuticle scale edges.

Due to the random nature of the scattering and reflection process leading to diffuse reflection and due to the non-uniform nature of the effect, the mean receptor angle γ_d

for diffusely reflected light may be expected to coincide with the incident angle of 40°, so that:

$$\gamma_d = \epsilon_I \tag{2}$$

A further part of the incident beam is refracted into the fiber according to Snell's or Descartes' law. Taking the cuticle inclination angle into account, this yields the relationship:

$$n_K = \sin(\epsilon_I - \phi)/\sin(\epsilon_R - \phi) \tag{3}$$

so that

$$\epsilon_R = \sin^{-1}[1/n_K \sin(\epsilon_I - \phi)] + \phi \tag{4}$$

where ϵ_R is the refraction angle, that is, the angle at which the light enters the fiber with respect to the normal direction and n_K is the refractive index of keratin, taken as n_K = 1.55 (11). Together with the values ϵ_I = 40° and ϕ = 2.5°, as given above, equation 4 yields ϵ_R = 26°.

Inside the hair the light is scattered and partly absorbed by hair pigment and color and is thus wavelength-filtered, depending on the hair color and its intensity. Diffuse reflection takes place at structural inhomogeneities within the cortex. For lightly colored hair, light may be diffusely reflected (11) at or in the medulla, a more or less continuous and hollow, tube-like structure in the fiber interior. An increase in this type of light reflection is considered to play an important role in loss of shine in lightened Japanese hair (13).

In very blonde or white hair a significant amount of light may be reflected at the backside of the fiber, which is the hair/air interface opposite to the point of incidence. Assuming that the light passes through the fiber axis (symmetrical passage) and taking the opposite tilt direction of this reflecting surface into account, the *b*ack-side reflection will occur at:

$$\gamma_b = \epsilon_R + 2\phi \tag{5}$$

yielding the expectation value γ_b = 31°.

This beam reaches the surface and, with the principles underlying equation 4, is refracted out of the fiber according to:

$$\gamma_i = \sin^{-1}[n_K \sin(\gamma_b + \phi)] - \phi \tag{6}$$

where γ_i is the receptor angle for this *i*nternally reflected light, with an expectation value of 55°. When this third component of light reemerges from the fiber, it has the color of the hair and is experimentally observed as a separate peak in the GP curve (1,2,4). Stamm *et al.* (11) consistently observed that the location of this peak was shifted to higher angles by 10%. Due to its width, the peak in the GP curve associated with this type of light is considered as being a specific fraction of diffusely reflected light, termed D_i, since it originates from *i*nternal reflection.

It is important to note that this model does not take into account the complex, layered morphological structure of the cuticle cell (10). Equal refractive indices are assumed for the morphological components. The two main components, namely exo- and endocuticle are indicated in Figure 4.

GP CURVE ANALYSIS

Figure 2 shows the raw data for the scattering profile of a dark brown, female, Caucasian hair near its root end. The data points show pronounced scattering due to the speckle effect, which results from the laser being a coherent monochromatic light source (1). To suppress the data scatter, moving average smoothing was found to be adequate, yielding the solid line in Figure 2, which is taken as the GP curve. The higher initial smoothness of scattering curves shown in the literature (e.g., 1,2,9) is attributed to the lower resolution of goniophotometric devices, the suppression of the speckle effect by the use of a white light source, and the testing of hair collectives.

Figure 5 shows the GP curve for a virtually black Asian hair. By fitting Gaussian peaks to the curves, as described below, it is shown that the curve prominently features a strong peak at a receptor angle of 36° and a width at half height of 9°. This peak is attributed to specular reflection. With equation 1 the location of this peak yields the tilt angle for the cuticle cells. The underlying, low-intensity, broad peak derives from diffuse reflection effects.

Figure 6 shows the GP curve of a medium brown hair, similar to the one for Figure 2, but measured at about 30 cm from the root. The curve shows a similar peak for specular reflection as the Asian hair, but superimposed on a broad background peak for D_S, that is, for diffuse scattering. Due to the lighter color of the hair closer to the tip compared to a position near its root end, a substantial fraction of the light enters the fiber, where it is not completely absorbed, but re-emerges in a diffuse manner. The D_S intensity shows a pronounced angular dependence with a directional preference of around 50°.

Figure 7 shows the GP curve for a light blonde hair, originating from the tip region of a light brown hair. The curve features the strong and narrow specular peak, superimposed on the strong, underlying intensity distribution of diffuse reflectance. A further peak is observed at 65°, which is attributed to D_i, that is, to internally reflected light.

The angle-dependent intensities of specularly (S), diffusely (D_s), and internally (D_i)

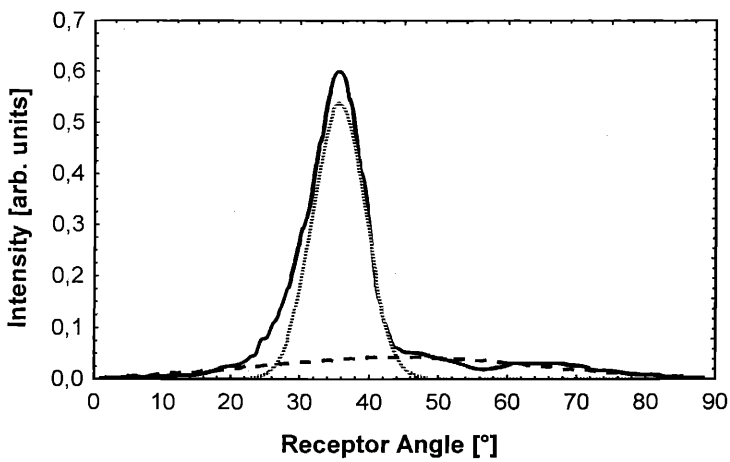

Figure 5. GP curve data (—) for a black Asian hair about 5 cm from its root end. Distributions for specularly (▪▪▪▪) and diffusely (---) reflected light, as fitted to the GP curve.

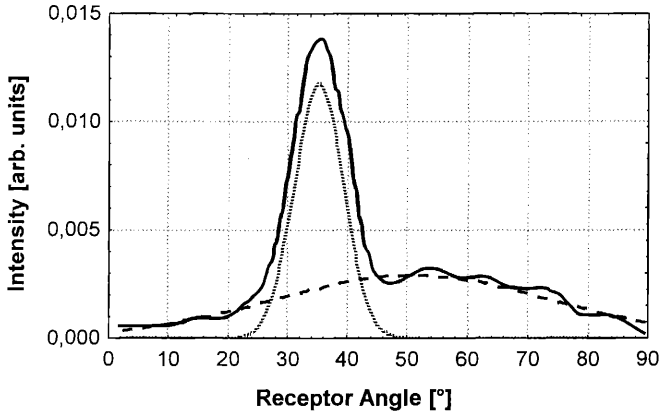

Figure 6. GP curve data (—) for a medium brown hair measured at a position of about 30 cm from the root. Distributions for specularly (▪▪▪▪) and diffusely (- - -) reflected light, as fitted to the GP curve.

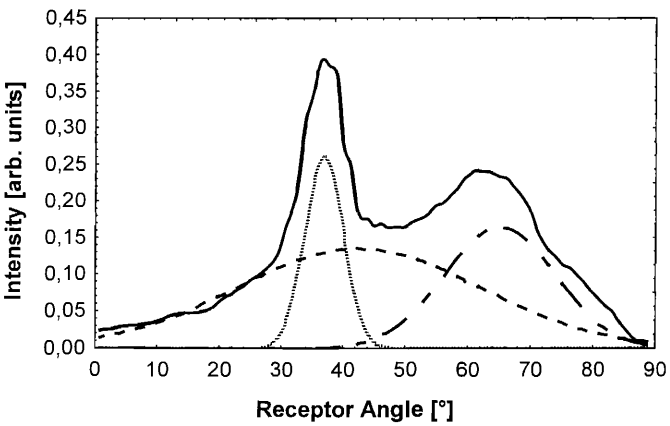

Figure 7. GP curve data (—) for a light blonde hair measured at a position near the tip end. Distributions for specularly (▪▪▪▪), diffusely (- - -), and internally (— -) reflected light, as fitted to the GP curve.

reflected light, respectively, are determined by simultaneously fitting to the GP curve up to three Gaussian distributions, each of which is given by:

$$I = A/[(2\pi)^{1/2}\sigma] \exp\{-\tfrac{1}{2}[(\gamma - \mu)/\sigma]^2\} \quad (7)$$

where I is the intensity count of a given type of reflected light at a given angle γ, σ is the standard deviation of the Gaussian distribution, describing its width, and μ its mean, signifying the position of the peak maximum. A is a scaling parameter related to the area of the peak.

The Gaussian peaks are fitted to the GP curves, applying nonlinear optimization strategies implemented in QuattroPro (Corel) and PeakFit (Jandel). The distributions are shown in Figures 5–7. The correlation coefficient, being the appropriate measure for the fraction of explained variance for the individual fits, always well exceeded 0.9.

The distributions are descriptions of the horizontal indicatrices (9) for the different fractions of light, reflected from a single hair. The choice of the Gaussian distribution

is an adequate, practical approach for the specular component, in view of the considerations by Guiolet *et al.* (4) and Rennie *et al.* (14).

In analogy to the approaches by Reich and Robbins (6) and Bustard and Smith (1) w_s, w_d, and w_i are introduced as parameters describing the width at half height of the Gaussian distributions for specularly, diffusely, and internally reflected light, respectively. The width at half height for a Gaussian peak is given by its standard deviation according to:

$$w = 2\sigma[2 \ln(2)]^{1/2} \tag{8}$$

Table I summarizes the locations (mean receptor angle) and widths of the Gaussian peaks for S and D_S for black Asian and brown and blonde Caucasian hair, respectively, and at five locations along their length. These were chosen such as to cover the individual lengths of the hair types. Cuticle scale angles were deduced from the location of the angular position of specularly reflected light, that is, from γ_s according to equation 1.

RESULTS AND DISCUSSION

By fitting Gaussian distributions to the GP curves, the locations and widths of the three types of reflected light were determined. From the location of the specular peak, fur-

Table I
Parameters for Specularly and Diffusely Reflected Light Derived From the GP Curves for Various Hair Types

Hair type	Position (cm)	N	Specular reflection γ_s (°)	Specular reflection w_s (°)	Cuticle angle (°)	Diffuse reflection γ_d (°)	Diffuse reflection w_d (°)
Black	1	12	35.7	10.3	2.13	43.3	43.7
	5	3	36.1	9.81	1.93	44.7	42.1
	10	7	34.2	10.7	2.91	35.2	52.7
	15	3	35.1	10.5	2.44	38.9	49.2
	20	7	34.0	10.1	3.01	37.1	48.9
Group mean ± q			35.0 ± 0.80	10.3 ± 0.62	2.50 ± 0.40	39.9 ± 2.09	47.2 ± 2.66
Brown	1	11	35.5	9.18	2.48	43.4	44.8
	10	9	38.1	9.70	1.27	47.0	48.7
	20	7	37.0	8.21	1.48	44.5	52.4
	25	4	34.5	10.2	2.76	44.0	53.6
	30	10	35.8	9.76	2.36	45.7	53.6
Group mean ± q			36.3 ± 0.81	9.35 ± 0.51	2.06 ± 0.39	45.1 ± 1.37	50.0 ± 2.28
Blonde	1	9	35.9	9.56	2.04	45.9	45.1
	5	9	36.4	9.32	1.79	45.3	45.5
	10	8	36.6	9.22	1.70	46.7	49.6
	15	9	37.2	8.40	1.40	45.5	46.1
	20	10	36.9	8.87	1.53	47.2	46.0
Group mean + q			36.6 ± 0.47	9.07 ± 0.66	1.70 ± 0.24	45.9 ± 0.96	46.4 ± 1.49
Grand mean ± q			36.0 ± 0.40	9.50 ± 0.35	2.05 ± 0.20	44.0 ± 0.92	47.9 ± 1.20

A number of hairs (N) were measured at various positions relative to the root. For some of the variables, a small number of obviously outlying data was removed (see text). Group and grand mean values are given with their 95% confidence range, q.

thermore, the tilt angle of the cuticle scales with respect to the fiber axis (cuticle angle) was derived.

By far, most GP curves could well be analyzed by the two-component approach, with a narrow peak attributed to specular and a broad peak to diffuse reflection, respectively. Only for the very blonde hair, D_i, as a further component of diffuse reflection, had to be considered.

All data were checked for outliers, prior to further analysis, by assessing them in so-called normal probability plots as implemented in the applied statistics software (15). In this type of plot, cumulative data frequencies follow a straight line, when the data are normally distributed. A small number of obvious outliers was readily identified (<10%) in these plots and was removed prior to further analysis of the parameter values. For the cuticle angle, a small number of data (<10%) with negative values were removed on the basis of physical implausibility.

The data given in Table I represent the accepted data and are arithmetic means for measurements taken at a given position on a number of hairs (N) of the same type. For a given hair type, the data are summarized in group means. For a given parameter, data are further summarized over all hair types in the form of grand means.

Effects of measurement position and hair type on the parameters were assessed for significance by analysis of variance (ANOVA) and linear regression (LR). In those cases where ANOVA indicated inhomogeneity, multiple comparison of means analysis was conducted, applying the nonconservative LSD test (15). The statistical significance of effects (ANOVA: inhomogeneity of data; LSD: differences between data groups; LR: slope of regression line) is characterized throughout by the α-value (16), which is the probability of committing a so-called type I-error, namely, by finding an effect that in fact does not exist. In cases where $\alpha < 0.05$, effects are significant at the usual 95% level and beyond.

SPECULAR REFLECTION AND CUTICLE ANGLE

With an angle of incidence of 40° on the hair for light traveling in the root-to-tip direction, the data in Table I show that the angular position of specularly reflected light is, as expected from the surface structure of human hair (see Figures 3 and 4), systematically shifted to 36° (grand mean). From the results for the receptor angle given by the angular position of the peak for the specular component γ_s, cuticle angles were derived according to equation 1 and are summarized in Table I.

There are some apparent changes of cuticle angles along the hair length, namely, a slight increase towards the tip for black hair (LR: $\alpha = 0.07$), no change for brown hair (LR: $\alpha = 0.85$), and a slight decrease for blonde hair (LR: $\alpha = 0.09$). Though none of this is really pronounced, such as being statistically significant at the 95% level, the results are considered to reflect the two counteracting effects of hair grooming, namely, cuticle lifting on the one hand and polishing through abrasion on the other (10,17–19), depending on hair diameter, cross-sectional shape, and length.

The results for the three hair types are summarized in Figure 8 in the form of a box-and-whisker plot. Analysis of variance shows that the data are inhomogeneous well beyond the 95% level ($\alpha = 0.005$), where the LSD test identifies the α levels for the differences,

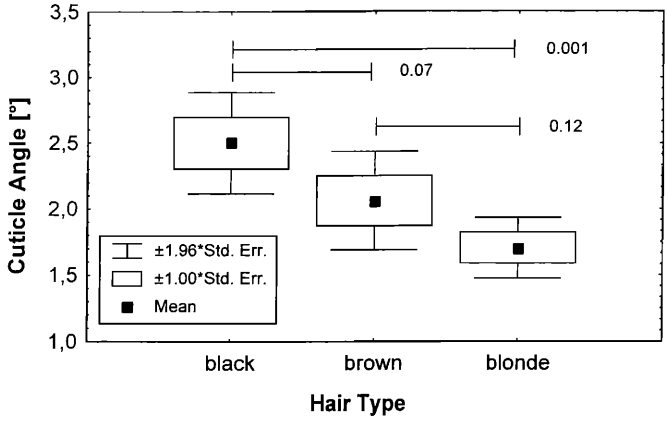

Figure 8. Box-and-whisker plot summarizing cuticle scale angles for the three hair types. Data points, boxes, and whiskers are defined by the arithmetic group means (Mean), the standard errors (Std. Err.), and the expectation values for the 95% confidence limits (1.96*Std. Err.). The horizontal whiskers signify a specific comparison of means (LSD test) given with the α-value to characterize the significance of the difference.

as given on the horizontal whiskers in Figure 8. Here it is shown that the cuticle angle decreased from black over brown to blonde, with all differences having relevant significance levels. The cuticle angle for the black hair (2.5°) is in good agreement with literature data between 2.5° and 3° (1,4,11). The values for brown and blonde hair are appreciably lower.

WIDTH OF SPECULAR PEAK AT HALF HEIGHT

As can be derived from the data underlying Table I, the width of the specular peaks at half height w_s shows for none of the hair types a dependence on the measurement position along the hair. Thus, no continuous influence of hair grooming, that is, from root to tip, can be detected through this parameter. This is despite the fact that the blonde hair was considerably longer (30 cm) compared to the other ones (20 cm) and changed its color from medium to light blonde from root to tip.

The results are summarized for the three types of hair in Figure 9 in the form of a box-and-whisker plot. The means show some variability (see Table I), where, as analysis of variance shows, inhomogeneity is significant at the 95% level ($\alpha = 0.02$). The LSD test yields the confidence levels on which the individual differences are statistically significant (see Figure 9). On this basis, only the differences between the black hair, on the one hand, and the two other hair types, on the other, are significant at the 95% level. The overall results indicate, nevertheless, that the width of the specular peak decreases with an increase in lightness of hair color.

The data for w_s yield a grand mean of 9.5 ± 0.35° (95% confidence limits; see Table I). This value is higher than the value Bustard and Smith (1) determined for gold-coated or black hair (8.3°) but lower than their value for brown hair (10.8°). This indicates that the origin of the specular reflected light is largely from near the very surface of the hair, irrespective of hair color. The decrease of width with increase of lightness may be a genuine effect, related to differences in the cuticle angle distribution. The authors, at

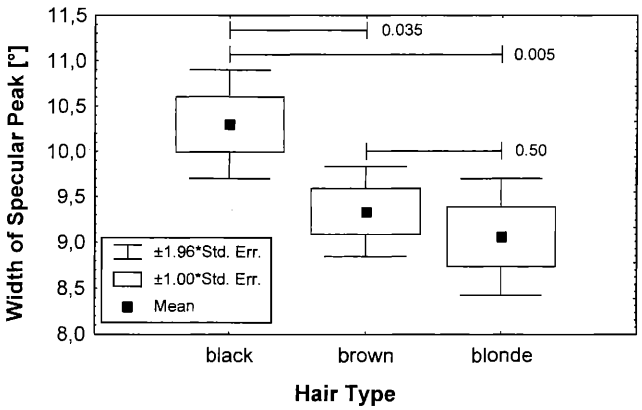

Figure 9. Box-and-whisker plot, summarizing the values for the width of the specular peak at half height, w_s, for the three hair types (see Figure 8).

this stage of the investigation, would tend to assume, however, that the effect is related to a tendency of the fit algorithms to detect narrower distributions for specularly reflected light with decreasing prominence of the related peak in the GP curve. Generally, the width of the specular peak for a given type of hair is a measure of the distribution of cuticle angles and can serve to assess surface damage, for a hair before and after a cosmetic treatment.

LOCATION OF THE DIFFUSE REFLECTION PEAK

For an ideal diffuse reflector, diffuse backward scattering would be uniform in intensity. With the strong directional component for this type of light, this condition is obviously not fulfilled for the surface of hair.

The results in Table I for the different fiber types at their root ends (1 cm), where all hairs are largely undamaged, show values between 43° and 46° that are not significantly different (ANOVA: α = 0.64). The values are higher than those of the respective receptor angles for specular reflection (35°–36°) and even higher than that of the expected receptor angle for a flat, specularly reflective surface (40°).

For the black, Asian hair the group means for the position of the peak location for diffuse reflection is 40° (see Table I). This effect is due to the fact that γ_d decreases significantly from root to tip (LR: α = 0.006; see Figure 10), paralleled by possibly a slight increase in the cuticle angle, as discussed above. There appears no straightforward explanation for this phenomenon, apart from the assumption that it is related to systematic and antagonistic changes of the hair surface due to grooming.

For the brown hair the receptor angle for diffuse reflections remains unchanged along the hair (ANOVA: α = 0.4), yielding a group mean of 45° ± 1.4°. The apparent shift of γ_D to higher angles for the blonde hair (see Figure 10) is not significant (LR: α = 0.16), yielding the group mean of 46° ± 1°, which is not significantly different from that for the brown hair (LSD: α = 0.44).

The 5°–6° shift of the diffuse reflection peak with respect to the expectation value of 40° is attributed to the fact that diffuse reflection mainly occurs at various locations near the

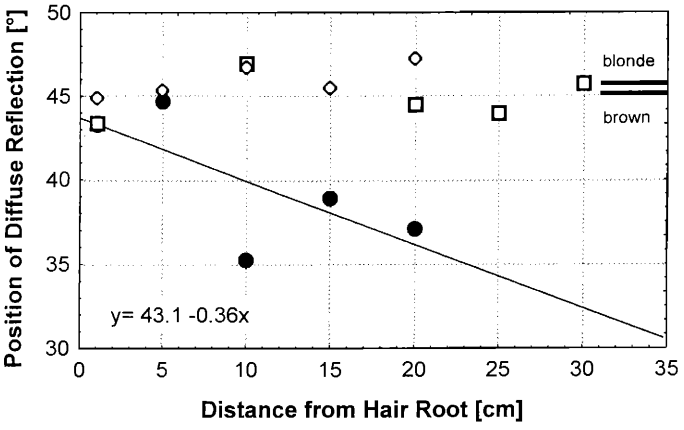

Figure 10. Means for the position of the diffuse reflection peak at half height, γ_d, at various positions along the hair, given as distance from the hair root. ● black hair, □ brown hair, ◇ blonde hair. The solid line is the linear regression line through the data for black hair, for which the equation, relating to all individual results, is given on the graph. The horizontal lines on the right mark the group means for brown and blonde hair, respectively (see Table I).

fiber surface, that is, in the multilayered structure of the cuticle, where systematic and pronounced differences in the refractive index and/or gaps between the cuticle layers are expected to play an important role (11). It is interesting to note, however, that this effect is similar in size but opposite in direction to the shift of the specular reflection angle, due to the cuticle inclination. This effect will be the objective of further investigations.

WIDTH OF THE DIFFUSE REFLECTION PEAK

The diffuse peaks show very similar overall widths, with group means between 47° and 50°, thus being, by a factor of about five, broader than the specular peak (see Table I).

For the black Asian hair this width shows an apparent slight increase from root (43.7°) to tip (48.9°), where the slope of the linear regression line just misses to be significant at the 95% level (α = 0.053). This effect corresponds to the systematic decrease of γ_d towards the tip region for this type of hair. The data are summarized in Figure 11.

For the brown hair, w_d increases significantly from root to tip (LR: α = 0.002). The regression line through the data is shown in Figure 11. For the black and the brown hair, where diffuse reflection will mainly occur at or close to the fiber surface, this change in the width of the related peak is attributed to increased damage of the hair from root to tip due to grooming, which leads to damage to the cuticle edges, chipping of exocuticle, and exposure of rough fracture surfaces in the endocuticle (10). For the blonde hair, the width of the diffuse reflectance peak has a group mean of 46.4° and is independent of the position on the hair.

Analysis of variance shows that group-wise there are significant differences between the

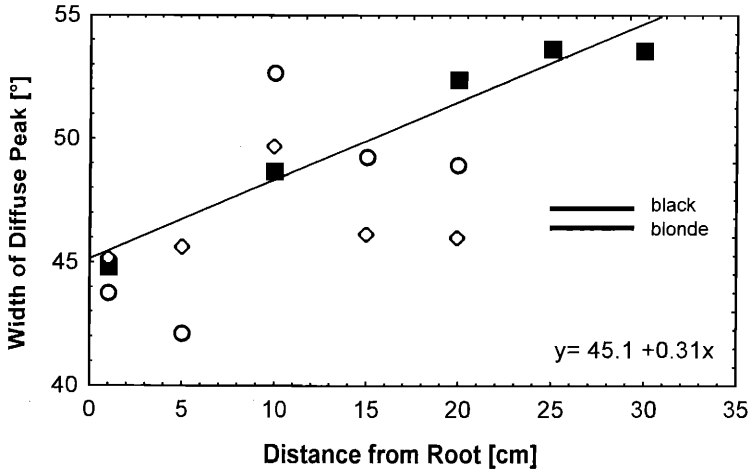

Figure 11. Means for the width of the diffuse reflection peak at half height, w_d, at various positions along the hair, given as distance from the hair root. ○ black hair, ■ brown hair, ◇ blonde hair. The solid line is the linear regression line through the data for brown hair, for which the equation, relating to all individual results, is given on the graph. The horizontal lines mark the group means for black and blonde hair, respectively (see Table I).

hair types (ANOVA: $\alpha = 0.03$). This inhomogeneity originates from the w_d values of the brown and the blonde hair being significantly different (LSD: $\alpha = 0.011$).

LOCATION AND WIDTH OF THE INTERNAL REFLECTION PEAK

A second, broader peak besides the one for specular reflection was observed in a comparatively small number of cases when measuring in the lightly colored tip region of the blonde hair. This peak is attributed to internal reflection. The frequency of occurrence of the effect was, in our experiments, much lower than would have been expected from the work of Stamm *et al.* (2,11).

The location of this peak, given by $\gamma_i = 64.0° \pm 2.96°$ (N = 8), is significantly shifted towards higher angles compared to the ray-tracing prediction (55°). This deviation is in good agreement with the observations by Stamm *et al.* (11) and is attributed to the repeated passage of the refracted and then internally reflected light through sheets of lower and higher refractive index. They propose, as a primary source of the effect, the existence of gaps between cuticle layers. In view of the highly cooperative structure of the hair cuticle, which on straining delaminates from the cortex in rings rather than in sheets within the cuticle layers (20), we are rather inclined to assume systematic differences in the refractive properties of the layered morphological structure of the cuticle cell, namely exo- and endocuticle. In this context, the large differences in the moduli of exo- and endocuticle, determined by Parbhu *et al.* (21), using atomic force microscopy, should be noted. Similar considerations apply for the shift of the peak for diffuse reflection, as discussed above.

The width of the peak for internally reflected light w_i is 24.9° ± 3.02°. Due to the nature of this light, this value is, not unexpectedly, by about a factor of roughly two, higher than that for the specularly reflected light and by the same factor smaller than the width of the diffuse peak in the GP curve.

CONCLUSION

The high-resolution, optical probing of the surface and interior of a hair fiber is enabled by fast data acquisition through simultaneous multi-angle goniophotometry, which gives quick access to the light reflection curve of a single hair at any given position along its length.

By fitting up to three Gaussian peaks to the GP curve, the different types of reflected light are determined with respect to their receptor angles and intensity distributions. From the data, detailed insight into the reflection of light from hair and its changes along the hair length are gained. Specific changes of the parameters are observed for the three hair types and along the hair length that can be attributed to the antagonistic effects of hair damage and grooming as well as to other phenomena that are currently not well understood. The next, immediate step of these investigations is to derive a measure of luster for human hair from the observations on light reflection (22).

REFERENCES

(1) H. K. Bustard and R. W. Smith, Studies of factors affecting light scattering by individual human hair fibres, *Int. J. Cosmet. Sci.,* **12,** 121–133 (1990).
(2) R. F. Stamm, L. M. Garcia, and J. J. Fuchs, The optical properties of human hair. II. The luster of hair fibers, *J. Soc. Cosmet. Chem.,* **28,** 601–609 (1977).
(3) M. Haller, H. Schmidt, and G. Sendelbach, Measurement of the optical paths of light in hair, Poster 42, *Proc. 21st IFSCC Int. Congress*, Berlin, 2000.
(4) A. Guiolet, J. C. Garson, and J. L. Levecque, Study of the optical properties of human hair, *Int. J. Cosmet. Sci.*, **9,** 111–124 (1987).
(5) Y. Tango and K. Shimmoto, Development of a device to measure human hair lustre, *J. Cosmet. Sci.,* **52,** 237–250 (2001).
(6) C. Reich and C. Robbins, Light scattering and shine measurements of human hair: A sensitive probe of the hair surface, *J. Soc. Cosmet. Chem.*, **44,** 221–234 (1993).
(7) W. Haertl, R. Klemp, and H. Versmold, Crystallization and characterization of crystallites in charge stabilized suspensions, *Phase Transitions,* **21,** 229–235 (1990).
(8) R. F. Schmidt and G. Thews, Eds., *Physiologie des Menschen* (Springer-Verlag, Berlin, 1995), Chapter 16.
(9) W. Czepluch, G. Hohm, and K. Tolkiehn, Gloss of hair surfaces: Problems of visual evaluation and possibilities for goniophotometric measurements of treated strands, *J. Soc. Cosmet. Chem.*, **44,** 299–318 (1993).
(10) J. A. Swift, Human hair cuticle: Biologically conspired to the owner's advantage, *J. Cosmet. Sci.,* **50,** 23–47 (1999).
(11) R. F. Stamm, M. L. Garcia, and J. J. Fuchs, The optical properties of human hair. I. Fundamental considerations and goniophotometer curves, *J. Soc. Cosmet. Chem.,* **28,** 571–599 (1977).
(12) E. Schulze zur Wiesche, *Untersuchungen zur haarpflegenden Wirkung von Henna,* MSc Thesis, Aachen University of Technology, 1995.
(13) S. Nagase, S. Shibuichi, K. Ando, E. Kariya, M. Okamoto, R. Yakawa, A. Mamada, and N. Satoh, Light scattering control at the medulla enhances human hair shine: Internal structures of hair fiber and its shine, *Proc. 21st IFSCC Int. Congress,* Berlin, 2000, pp. 153–159.
(14) J. H. S. Rennie, S. E. Bedford, and J. D. Hague, A model for the shine of hair arrays, *Int. J. Cosmet. Sci.,* **19,** 131–140 (1997).
(15) *Statistica for Windows* (computer program manual) (StatSoft Inc., Tulsa, OK, 1999).
(16) J. H. Zar, *Biostatistical Analysis* (Prentice Hall, NJ, 1996).
(17) M. L. Tate, Y. K. Kamath, S. B. Ruetsch, and H.-D. Weigmann, Quantification and prevention of hair damage, *J. Soc. Cosmet. Chem.,* **44,** 347–371 (1993).

(18) M. Gamez-Garcia, The cracking of human hair cuticles by cyclic thermal stresses, *J. Soc. Cosmet. Chem.*, **49**, 141–153 (1998).
(19) M. L. Garcia, J. A. Epps, R. S. Yare, and L. D. Hunter, Normal cuticle-wear patterns in human hair, *J. Soc. Cosmet. Chem.*, **29**, 155–175 (1978).
(20) G. H. Henderson, Fractography of human hair, *J. Soc. Cosmet. Chem.*, **29**, 449–467 (1978).
(21) A. N. Parbhu, W. G. Bryson, and R. Lal, Disulfide bonds in the outer layer of keratin fibers confer higher mechanical rigidity: Correlative nano-indentation and elasticity measurement with an AFM, *Biochemistry*, **38**, 11755–11761 (1999).
(22) F.-J. Wortmann, E. Schulze zur Wiesche, and B. Bourceau, Analyzing the laser-light reflection from human hair fibers. II. Deriving a measure of luster, *J. Cosmet. Sci.*, in preparation.